JOURNAL OF MATERIALS SCIENCE 39 (2004) 6957–6964

Quantitative analysis of grain size in bimodal powders by x-ray diffraction and transmission electron microscopy

J. HE, J. YE, E. J. LAVERNIA
Department of Chemical Engineering and Materials Science, University of California, Davis, Davis, CA 95616-5294, USA

D. MATEJCZYK, C. BAMPTON
Rocketdyne Propulsion & Power, Boeing, Canoga Park, CA 91309-7922, USA

J. M. SCHOENUNG*
Department of Chemical Engineering and Materials Science, University of California, Davis, Davis, CA 95616-5294, USA
E-mail: jmschoenung@ucdavis.edu

In most studies related to milled powders, the grain size[1] is analyzed via X-ray diffraction (XRD) experiments, and a transmission electron microscopy (TEM) image with high magnification, if provided, is used primarily to confirm the results obtained by XRD experiments. This widely used approach is reasonable in light of the difficulties associated with TEM sample preparation. The present study, however, addresses the hypothesis that such an approach may not be valid when there is an inhomogeneous distribution of grains present. TEM examination, carried out in carefully prepared Al-7.5 wt% Mg samples, in which a global region is observable by TEM, provided the opportunity for quantitative analysis of grain size in cryomilled powders having an inhomogeneous distribution of grain sizes. The cryomilled Al-7.5 wt% Mg had a bimodal grain microstructure of 77% (area fraction) fine grains in the range of 10 to 60 nm and 23% coarse grains of approximately 1 μm. The results show that the XRD analysis yields a grain size that is close to that present in the fine-grained regions (i.e., 10–60 nm). The present study also systematically investigated the influence of the nine possible combinations of the Cauchy (C) and the Gaussian (G) approximations on the calculated grain size value, and the results show that the CC-CC approximation resulted in the largest calculated grain size, the GG-GG generated the smallest one, and the CG-CG, the approximation recommended by Klug and Alexander [1], led to a calculated grain size that is approximately equal to the average one from the CC-CC and GG-GG approximations. The maximum possible fluctuation of grain size values stemming from the various approximations is 38%.

1. Introduction

X-ray diffraction (XRD) and transmission electron microscopy (TEM) are widely used to carry out quantitative analyses of grain size and grain size distributions of nanostructured materials (e.g., 5–100 nm). A few excellent studies [2–5] have been carried out to evaluate the grain size of nanocrystalline materials, on the basis of the fundamental theories for XRD analysis of grain size. In XRD analyses, any diffraction peak line broadening that results from crystallites with grain sizes in excess of 100–300 nm is considered to be negligibly small [1]. This implies that the XRD analysis is not suited for grain size evaluation in materials having a grain size that exceeds 100 nm. Inspection of the available literature shows that milling processes are frequently used to synthesize nanocrystalline powders [6–10]. In this process, a repeated cold welding, fracturing of powder particles occurs under a highly energetic ball charge, and coarse grains are gradually refined with increasing milling time [11, 12]. The stochastic nature of most widely used milling processes raises the possibility that the distribution of grain sizes will not be homogenous. In other words, a nano-structure (i.e., the grain size is less than 100 nm) may be attained in some areas, whereas other regions will retain a coarse-grained character. Such a mixed grain size configuration and basic information on the stochastic nature of the milling process has

*Author to whom all correspondence should be addressed.
[1]The phrase "grain size" indicates the average value of the grain diameter.

received only limited attention. In 1999, Tellkamp *et al*. [13] argued that in fact such a distribution of grain sizes was attractive from a mechanical behavior standpoint, because the large grains accommodate plasticity (i.e., dislocation behavior), whereas the nano-grains provide strengthening and other desirable mechanical properties. Subsequent studies by Witkin *et al*. [14] and Wang *et al*. [15] showed that in fact this characteristic could be used to design materials with unique combinations of strength and ductility. Accordingly, the objective of the present investigation was to provide insight into the quantitative analysis of grain size in milled powders where grains might be inhomogeneously distributed.

2. Experimental procedure

Spray-atomized Al-7.5 wt% Mg powder was employed as the starting material for cryomilling (cryogenic mechanical milling, in which the liquid nitrogen is introduced directly into the milling chamber, is referred to as cryomilling [11]), with a modified Union Process 1-S attritor at a rate of 180 rpm in a stainless steel tank with stainless steel balls maintained at 100 K, for 8 h. The ball-to-powder weight ratio was 32:1. XRD measurements were performed using Cu K_α ($\lambda = 0.15418$ nm) radiation in a Siemens D5000 diffractometer equipped with a graphite monochromator. A low scanning rate 0.12 degrees/min. was used to ascertain the accuracy of the measurements. After the pattern effects of $K_{\alpha 2}$ were subtracted, the peak position, full width at half maximum (FWHM), and integral width (IntW) of XRD reflections were computed using a software package available with the Siemens D5000 diffractometer. TEM studies were conducted on a Philips CM 20 microscope operated at 200 keV. To achieve a sufficiently large TEM observable area (more than twenty entire powder particles), the TEM samples were prepared using the following procedure [16]. The powders and epoxy were mixed to create a slurry, which was then mounted into a nut. The nut was prepared by slicing a section from a stainless steel tube. The tube, and therefore the nut, had an outside diameter of 3 mm and inside diameter of 2 mm. The resulting TEM sample was thus a 3-mm diameter disk. The disk was ground and then dimpled to approximately 30 μm thick using a dimpler fitted with diamond grinders. The particle size of the diamond grinders descended from a 3 μm grade down to a 1 μm grade. The final thinning perforation process was carried out using a Gatan 600 argon ion mill at a temperature near that of liquid nitrogen (the extension of the copper sample stage was soaked in liquid nitrogen) with an angle range from 22 to 10°.

3. Results and discussion

3.1. XRD analysis of the cryomilled Al-7.5 wt% Mg powder

Fig. 1a depicts the X-ray diffraction peaks from the {111} plane for both annealed (heated to 460°C, and held for 4 h in argon, then slowly cooled down to room temperature) and cryomilled Al-7.5 wt% Mg powder. To illustrate schematically the change in the sharpness/width of the XRD reflections visually, the $K_{\alpha 2}$ peak is included in the spectrum shown in Fig. 1a, although the pattern of $K_{\alpha 2}$ was subtracted in the following calculation of grain size and microstrain. The XRD peak for the cryomilled powder broadens and the height decreases drastically. In contrast to the XRD peak for the annealed sample, the peak that originated from $K_{\alpha 2}$ in the spectrum of the cryomilled powders cannot be visually distinguished as a result of the broadening of the reflections caused by cryomilling.

In order to estimate the grain size in the cryomilled Al-7.5 wt% Mg powder, established methods were used [1]. These methods require the definition and use of several terms. Here, β_m is the angular full width at half-maximum (FWHM) of the measured diffraction peaks for the cryomilled sample, and β_a is the FWHM of the diffraction peaks for the standard sample (the annealed sample). δ_m is the integral width of the diffraction peaks (IntW) for the cryomilled sample, and δ_a is the IntW for the annealed sample. The values of β_m, β_a, δ_m, and δ_a are computed using the software package available with the diffractometer used. The measured profile is a convolution of the instrumental broadening (the broadening from the instrument itself) profile and the intrinsic broadening (stemming from small grain size and microstrain) profile. Subtraction of the influence of the instrumental broadening was made on the basis of an assumption regarding the shapes of the intrinsic profile and instrumental profile, as presented here. The two most commonly assumed line shapes of XRD profiles are the Gaussian, $f(x) = f_0(x)\exp(-k^2x^2)$, and the Cauchy, $f(x) = f_0(x)/(1+k^2x^2)$ [1], shown in Fig. 1b. If the intrinsic and instrumental profiles (the latter is represented by the measured profile of the annealed sample) are assumed to be Cauchy-Cauchy (CC), Gaussian-Gaussian (GG) or Cauchy-Gaussian (CG), respectively, the following equations are obtained [1].

$$\beta = \beta_m - \beta_a \text{ or } \delta = \delta_m - \delta_a \quad (1)$$

$$\beta = \left(\beta_m^2 - \beta_a^2\right)^{1/2} \text{ or } \delta = \left(\delta_m^2 - \delta_a^2\right)^{1/2} \quad (2)$$

$$\beta = \beta_m - \beta_a^2/\beta_m \quad \text{or } \delta = \delta_m - \delta_a^2/\delta_m \quad (3)$$

From these three equations, the intrinsic FWHM (β) and IntW (δ) for the diffraction peaks were calculated and the results are listed in Table I.

The results shown in Table I quantitatively indicate a considerable broadening of the diffraction peaks for

TABLE I Full width at half-maximum (β) and integral width (δ) for the diffraction peaks in cryomilled Al-7.5 wt% Mg powder; the unit for 2θ, β, and δ is degree (°)

Approximation	*hkl*	111	200	220	113
	2θ	38.5	44.705	64.98	77.876
	β_m	0.399	0.457	0.573	0.691
	β_a	0.061	0.067	0.079	0.092
	δ_m	0.487	0.552	0.675	0.810
	δ_a	0.074	0.078	0.094	0.111
CC	$\beta = \beta_m - \beta_a$	0.338	0.390	0.494	0.599
GG	$\beta = (\beta_m^2 - \beta_a^2)^{1/2}$	0.394	0.452	0.567	0.685
CG	$\beta = \beta_m - \beta_a^2/\beta_m$	0.390	0.447	0.562	0.679
CC	$\delta = \delta_m - \delta_a$	0.413	0.474	0.581	0.699
GG	$\delta = (\delta_m^2 - \delta_a^2)^{1/2}$	0.481	0.546	0.668	0.802
CG	$\delta = \delta_m - \delta_a^2/\delta_m$	0.476	0.541	0.662	0.795

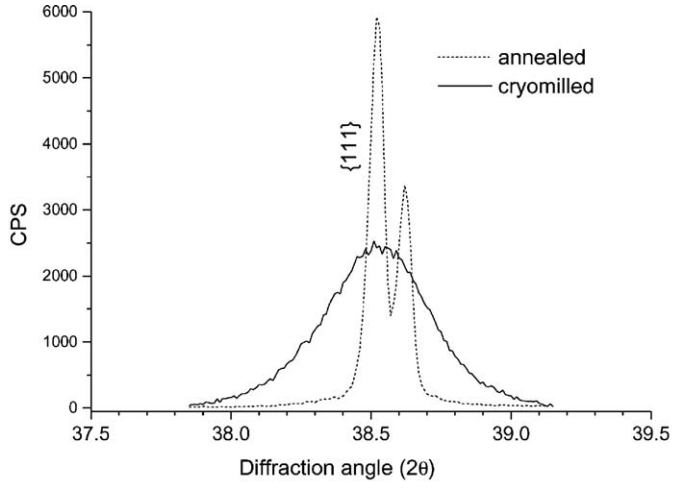

(a)

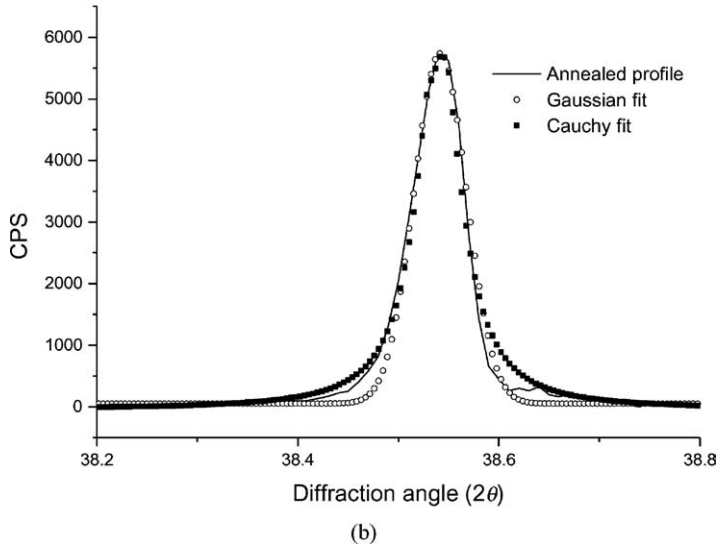

(b)

Figure 1 XRD profiles and the Gaussian and Cauchy approximations: (a) {111} XRD reflections for both annealed and cryomilled Al-7.5 wt% Mg alloy and (b) Gaussian and Cauchy approximations for annealed Al-7.5 wt% Mg alloy, {111} XRD reflection ($K_{\alpha 2}$ peak is subtracted).

the cryomilled powder relative to those for the annealed sample. The intrinsic broadening values calculated by the CC approximation are less than those by the GG approximation, which are very close to those by the CG approximation.

In milled powders, the overall intrinsic broadening of XRD reflections consists of those arising from both small grain size and microstrain. The overall integral intrinsic broadening profile is a convolution of the integral grain size broadening, δ_D, profile and the integral microstrain broadening, δ_S, profile [1]. Once again, the relationship among the grain size broadening, microstrain broadening and the overall intrinsic broadening is coupled to an assumption about the shapes of the grain size broadening profile and microstrain broadening profile. Suppose the grain size broadening profile and the microstrain broadening profile to be Cauchy-Cauchy (CC), Gaussian-Gaussian (GG) or Cauchy-Gaussian (CG), respectively, the following equations are obtained [4].

$$\delta = \delta_D + \delta_S \tag{4}$$

$$\delta = \left(\delta_D^2 + \delta_S^2\right)^{1/2} \tag{5}$$

$$\delta = \delta_D + \delta_S^2/\delta \tag{6}$$

The integral grain size broadening in the material can be expressed as

$$\delta_D = k\lambda/D\cos\theta \tag{7}$$

where $k = 1$, λ is the wavelength, in the case of Cu $K_{\alpha 1}$, $\lambda = 0.15406$ nm, θ is diffraction angle, and D is grain size [1]. The integral microstrain broadening can be written as

$$\delta_S = 4e\tan\theta \tag{8}$$

where e is an approximate upper limit of the lattice distortion [1].

Substituting Equations 7 and 8 into Equations 4–6, the following equations result:

$$\delta\cos\theta = 4e\sin\theta + k\lambda/D \tag{9}$$

$$\delta\cos\theta = [(4e\sin\theta)^2 + (k\lambda/D)^2]^{1/2} \tag{10}$$

$$\delta\cos\theta = k\lambda/D + 16\,e^2\sin^2\theta/\delta\cos\theta \tag{11}$$

For Equation 9, using the values of δ derived from Equations 1–3, as shown in Table I, $\delta\cos\theta$ is plotted against $\sin\theta$ for four XRD reflections. The data should be on a straight line, with a slope of $4e$ and an

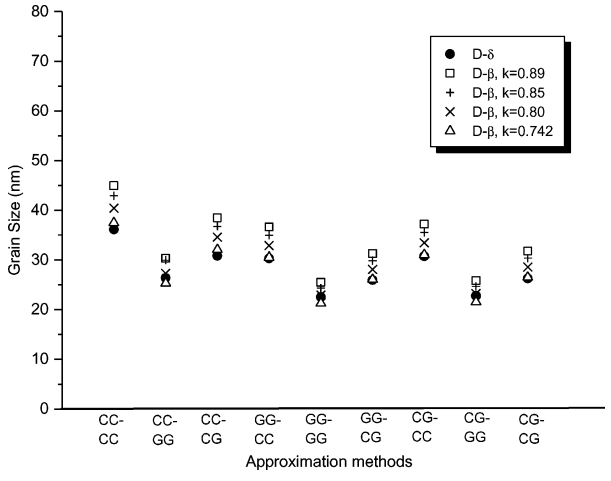

Figure 2 Influence of XRD profile approximation method on the calculated grain size of cryomilled Al-7.5 Mg powder. D-δ represents grain size value calculated from the integral width (δ), and D-βs designate the grain size values calculated from the full width at half maximum intensity (β). When $k = 0.742$, the grain sizes from the full width at half maximum intensity are close to those from the integral width, regardless of the approximation used. CC: Cauchy-Cauchy approximation; CG: Cauchy-Gaussian approximation; and GG: Gaussian-Gaussian approximation.

intercept of $k\ \lambda/D$. Similarly, when $\delta^2\cos^2\theta$ is plotted against $\sin^2\theta$ for Equation 10, the result should be a straight line, with a slope of $16e^2$ and an intercept of $(k\ \lambda/D)^2$; and when $\delta\ \cos\theta$ is plotted against $\sin^2\theta\ /\delta\ \cos\theta$ for Equation 11, the slope should be $16e^2$ and the intercept is $k\ \lambda/D$. Using this method, the data shown in Table I exhibit a good fit, with linear correlation coefficients (R) between 0.97 and 0.99. The calculated grain size and microstrain values for the cryomilled Al-7.5 wt% Mg powder are shown in Table II and Fig. 2.

From Table II and Fig. 2, it can be seen that when the CC approximation for calculating intrinsic broadening of XRD profiles is used, the values of grain size are larger than those when either the GG or the CG approximation is used. The values are nearly invariant when the CG results are compared with those using the GG approximation. It should be noted that, for a fixed δ value, the values of grain size and microstrain are complementary. Because the CC approximation results in large δ_D and small δ_S values, thus a large grain size and small microstrain are obtained when the CC approximation is used to do linear fitting for grain size and microstrain. The GG approximation leads to the smallest grain size and largest microstrain values, and cannot be replaced by the CG values, unlike in the calculation of the intrinsic broadening. The largest grain size value is devised from the CC-CC approximation, and the smallest one from the GG-GG approximation. Combining all of this, the maximum possible variation in calculated grain size value that can result from changing the approximation methods is 38% = [(maximum − minimum)/maximum].

According to Klug and Alexander [1], the shape of the intrinsic broadening profile is approximately the Cauchy, and that of the instrumental profile is approximately the Gaussian, hence, the broadening from the CG approximation should best represent the intrinsic broadening. The grain size broadening in a strained sample is in the form of the Cauchy, and microstrain broadening is Gaussian in form [1, 4]. Therefore, the CG approximation is the most appropriate method for the linear fitting for grain size and microstrain. The grain size and microstrain is 26.3 nm and 3.2%, respectively, by the CG-CG approximation. This grain size value is near the middle of the range of the maximum value obtained with the CC approximation, and the minimum value obtained with the GG approximation. This microstrain value is very close to the maximum value calculated with the GG-GG approximation.

As shown in Fig. 1b, the FWHM of a XRD profile can be accurately represented by both Gaussian and Cauchy functions, however, a real IntW is larger than that simulated by Gaussian function and smaller than that by Cauchy function. Therefore, the FWHM of the XRD profile is of interest. Although the linear fit method is initially derived from the integral width of XRD profile [1], as a comparison, the calculation of grain size and microstrain on the basis of the FWHM is also carried out, that is, using the values of β shown in Table I, a linear fit is determined on the basis of Equations 9–11, and the results are listed in Table II. In the calculation using the FWHM, the microstrain value is not influenced by the coefficient, k, which is influenced by the shape of the grains measured. Table II shows that microstrain values based on the FWHM and the IntW are close to

TABLE II Calculated grain size and microstrain of cryomilled Al-7.5 wt% Mg powder

	Basis: IntW (δ)			Basis: FWHM (β)		
Approximation[a]	Grain size (nm)	Microstrain (%)	Correl. coefficient	Grain size (nm)	Microstrain (%)	Correl. coefficient
CC-CC	36.16	2.060	0.985	44.96	2.009	0.992
CC-GG	26.39	2.965	0.987	30.34	2.684	0.992
CC-CG	30.84	2.894	0.971	38.49	2.709	0.980
GG-CC	30.33	2.285	0.987	36.63	2.194	0.991
GG-GG	22.53	3.355	0.988	25.51	3.011	0.992
GG-CG	25.96	3.252	0.974	31.27	3.002	0.980
CG-CC	30.73	2.274	0.987	37.23	2.187	0.992
CG-GG	22.78	3.331	0.988	25.85	2.992	0.992
CG-CG	26.29	3.232	0.974	31.81	2.998	0.981

[a]The first two letters designate the approximation for calculating intrinsic broadening of XRD profiles and the last two letters designate the approximation for linear fitting of grain size and microstrain.

each other. However, the much larger grain size values derived by using the FWHM, relative to those derived by using the IntW, are obtained when k is selected as 0.89, a value that is commonly used [1–4]. To investigate the influence of the value of k on the calculated value of grain size, alternative values of k were considered. The results indicate that when $k = 0.85$ and 0.80, the grain size values derived on the basis of the FWHM gradually approach those derived by using the IntW value, for all nine approximations used. Finally, when $k = 0.742$, the two grain size values are very close (the variation is less than 5%), see Fig. 2.

Although there is some variation in the values of grain size derived via the different XRD profile approximations presented above, all approximations indicate an average grain size between 20 and 50 nm. Using conventional interpretations, these results imply that the cryomilled Al-7.5 wt% Mg powder can be characterized as nanocrystalline because it exhibits a grain size in the range of 5–100 nm. However, the TEM results, as discussed in the section that follows, indicate that the results of XRD analysis carried out for the cryomilled Al-7.5 wt% Mg powder are misleading.

3.2. TEM analysis of cryomilled Al-7.5 wt% Mg powder

Fig. 3a and b show TEM image and diffraction patterns for the cryomilled Al-7.5 wt% Mg powder. Fig. 3a is a bright field TEM image, indicating that the powder contains both nanocrystalline grains and coarse grains. The inserted diffraction pattern, concentric diffraction rings representing polycrystalline and diffraction spots showing orientations of one coarse grain, from the area indicated by the letter A, clearly shows that the diffracted area is a mixture of fine grains and coarse grain. Fig. 3b is the corresponding dark field image formed using the $11\bar{1}$ diffraction spot, indicating the coarse grain having a dimension of 0.9 micron. This value is much larger than the grain size value determined by the XRD analysis. The inserted diffraction pattern taken from area B in Fig. 3a, indicates that grain B is an intact coarse grain having its [011] orientation parallel to the direction of the electron beam. The dark field image of grain B clearly shows the absence of subgrains or other domains within the grain. Therefore, the TEM examination verifies the inaccuracy of the XRD analysis for the cryomilled Al-7.5 wt% Mg powder.

The primary disadvantage of the application of TEM to grain size analysis has often been the claim that the volume of material that one can examine in TEM is always very small. This leads to the uncertainty as to whether a truly characteristic region of the sample has been investigated [3]. However, in a carefully prepared TEM sample following the procedure described above in the section on experimental procedure, a "global" sample region remained observable via TEM. In the present study, at least twenty entire powder particles were examined. Using low magnification, Fig. 4 shows TEM images of an entire particle agglomerate, revealing an inhomogeneous distribution of grain sizes. It should be noted that in Fig. 4 the particle agglomerate is smaller than the average for the material, which was approximately 40 μm. This view was chosen so that the entire particle could be viewed in one image at a proper magnification at which small grains are also observable. In Fig. 4a, the letters CAB indicate a large coarse-grained region composed of more than twenty grains having dimensions in the range from 0.5 to 2 μm. The letters D and E show discrete coarse grains. Fig. 4b is the corresponding dark field image.

With TEM images taken at both low and high magnifications, the grain size distribution of the cryomilled Al-7.5 wt% Mg powder was investigated and the results show that the powder was composed of 77% fine-grained regions (area fraction), in which grain sizes ranged from 10 to 60 nm, and 23% coarse-grained regions having a grain size of 0.5–2 μm, a statistical distribution of grain size on the basis of TEM dark field images is plotted in Fig. 5. A bimodal grain size distribution can be observed.

The present TEM results are quite straightforward. However, it should be noted that (1) in most of the related investigations, the grain size of milled powder has been analyzed using XRD, and TEM images, if provided, have been taken at relatively high magnification to demonstrate the morphology of the nanosized grains. The main purpose of TEM characterization was to confirm the XRD results. The results from the present study show that XRD does not provide a valid characterization for materials having an inhomogeneous distribution of grains, especially if the grains in certain regions are larger than 100 nm, which is beyond the range that XRD can measure (2). A bimodal characteristic in the grain size distribution does not necessarily mean an unsuccessful synthesis of a nanocrystalline material. In fact, it is highly desirable to have the flexibility to generate microstructures that contain multiple-scales, provided that these can be attained in a repeatable manner. Bulk multi-scale materials with high mechanical performance have been synthesized in our laboratory using the bimodal cryomilled powder [17]. Nanocrystalline regions lead to high strength and coarse-grained regions lead to high ductility.

The experimental results indicating that there was no evidence for X-ray diffraction from the coarse grains that TEM revealed to be present in the cryomilled Al-7.5 wt% Mg powder may be rationalized on the basis of the following three factors. (1) The coarse grains produce a very small profile broadening that is not measurable, thus the coarse grains have no contribution to the overall profile broadening. (2) There is a "shielding" phenomenon because most of the coarse grains are located in the "core" regions of the powder particles and are surrounded by a "shell" of nanocrystalline grains. The mass absorption coefficients, μ/ρ, of Al for Cu K_α radiation is 50.23 cm^2/g [18], if the density, ρ, is considered to be 2.70 g/cm^3. The penetration depth, x, of X-ray radiation, can be calculated by: $2\ \mu x/\sin\theta = \ln(1/1 - G_x)$ [18], where G_x is the attenuation fraction of the intensity, i.e., $G_x = 0.9$ represents that 90% intensity has been attenuated and 10% remains. If the thickness corresponding to 50% intensity is considered as the penetration depth of the X-ray,

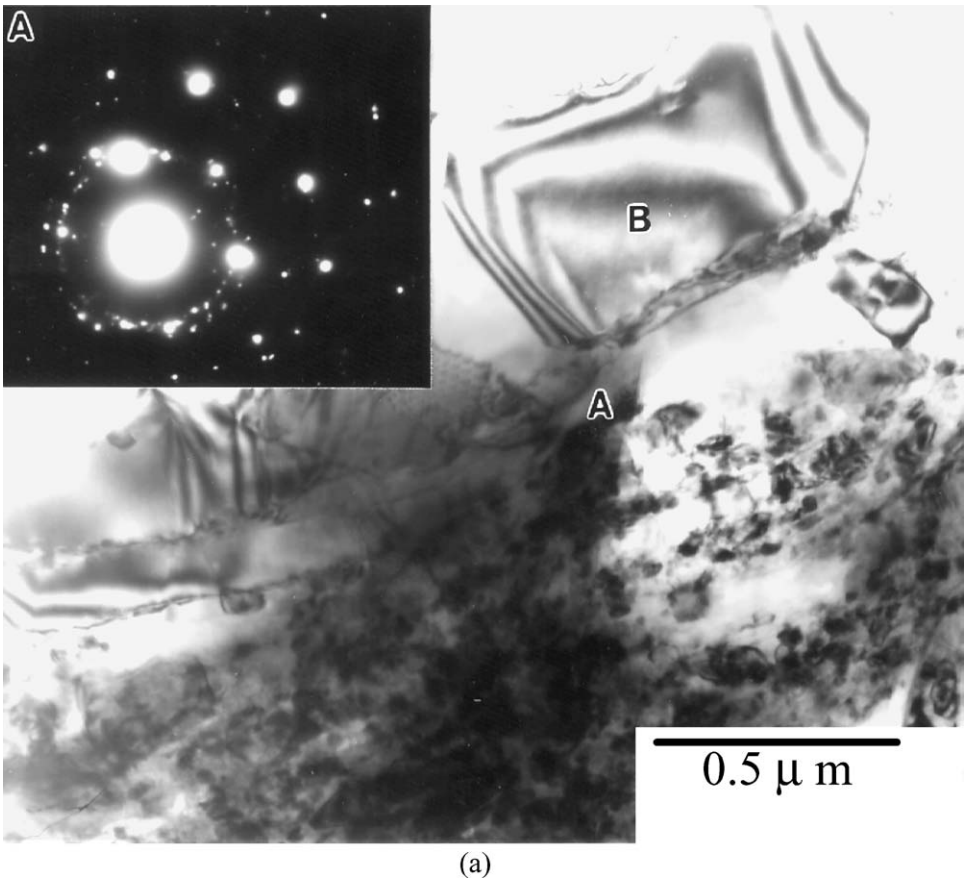

(a)

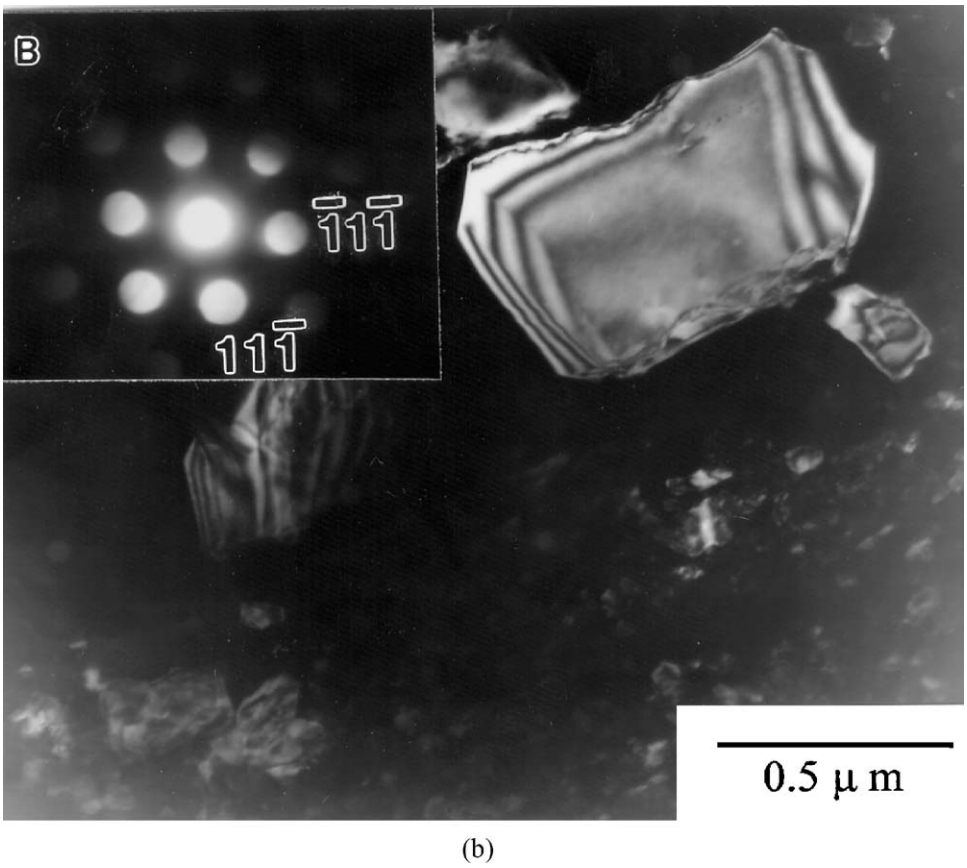

(b)

Figure 3 TEM images of the cryomilled Al-7.5 wt% Mg powder, indicating the presence of coarse grains: (a) TEM bright field image of the cryomilled Al-7.5 wt% Mg powder and (b) TEM dark field image of the cryomilled Al-7.5 wt% Mg powder, $B = [011]$; $g = 11\bar{1}$.

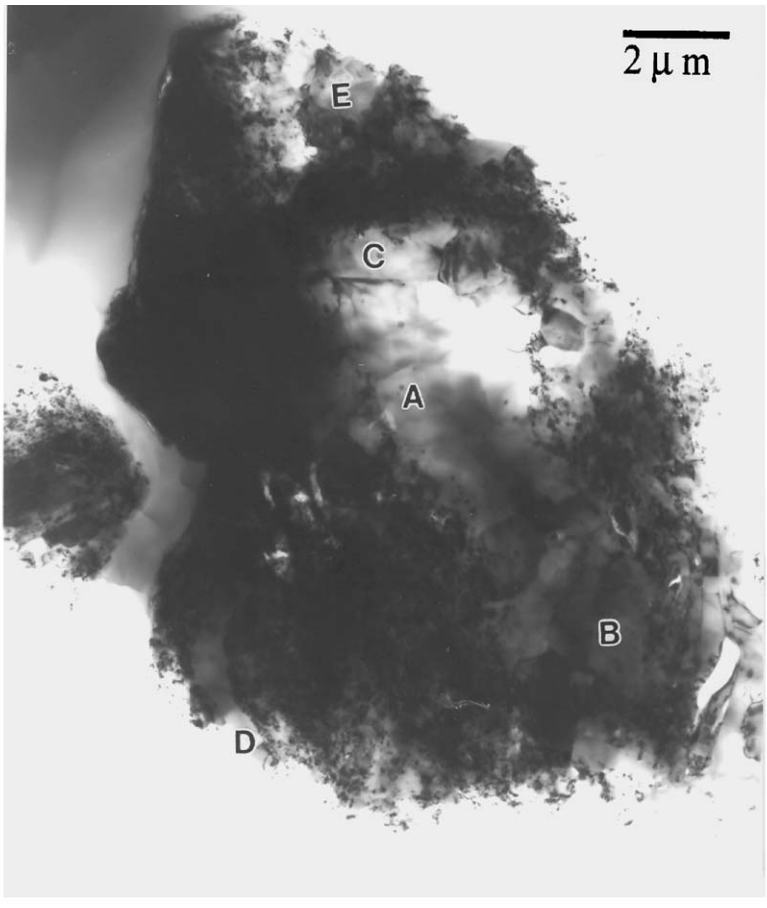

(a)

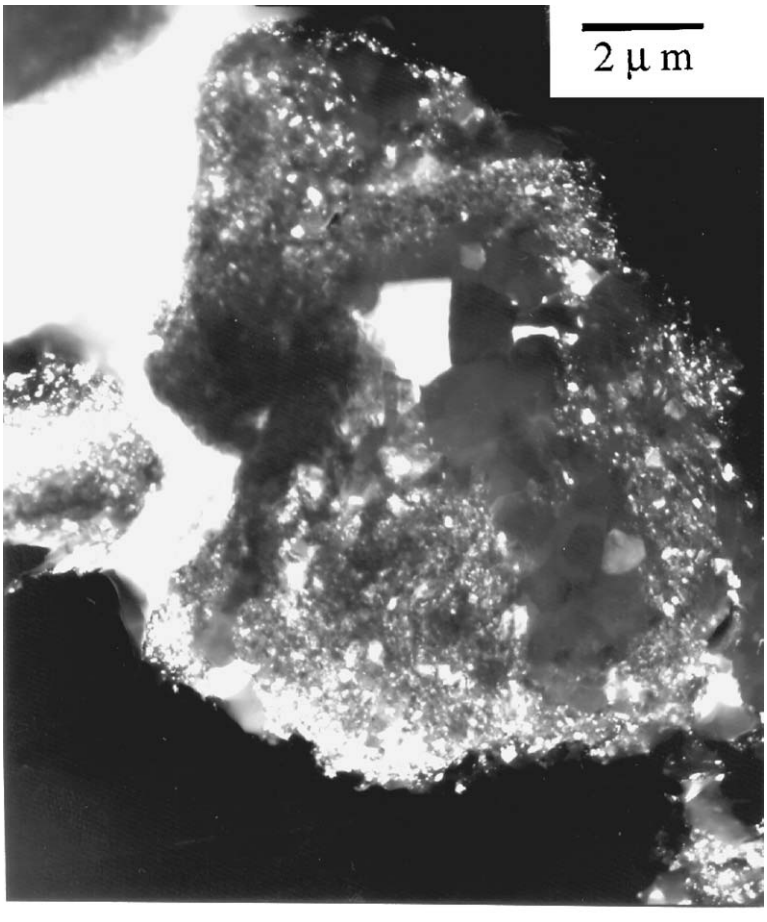

(b)

Figure 4 TEM images of an entire cryomilled Al-7.5 wt% Mg particle agglomerate, showing a bimodal distribution of grain size: (a) TEM bright field image of an entire cryomilled Al-7.5 wt% Mg particle agglomerate and (b) the corresponding dark field image, taken using {111} ring.

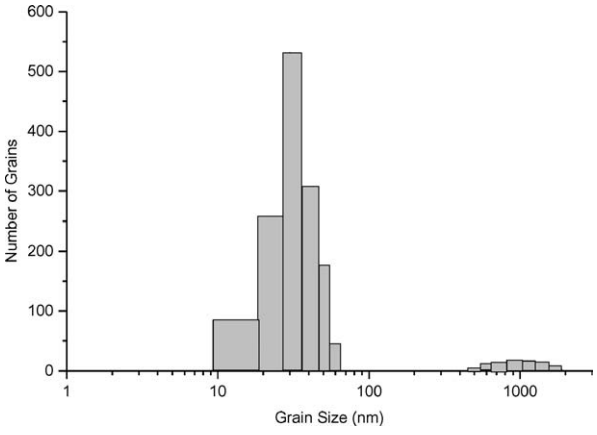

Figure 5 Distribution of grain size in cryomilled Al-7.5 Mg powder, as determined by TEM dark field images.

that is, taking $G_x = 0.5$, the penetration depth, x, is calculated to be 8.4 μm. Experimentally, the "shell" of nanocrystalline grains is observed to be approximately 5–10 μm thick. Therefore, the incident X-ray radiation for the core region is attenuated by about 50%. As a result, the scattering from the core is expected to be insignificant (3). The overall area fraction of coarse grains is only 23%. Considering the coarse grains as a phase and referring to the calculation for phase volume fraction using XRD analysis, it is likely that the contribution of the coarse grains to the intensity of the XRD profile can be completely hidden, because the contribution of the coarse grains to the XRD intensity is small and superimposed on the peak produced by the nanocrystalline grains.

4. Conclusions

The results of the present study are briefly summarized as follows:

1. XRD analysis indicated that cryomilled Al-7.5 wt% Mg alloy powder was nanocrystalline with an average grain size of approximately 26 nm. However, TEM, combining the examination at low and high magnifications, visually showed that the same powder had a bimodal grain size distribution of 77% fine grained regions (area fraction), in which the grain size ranged from 10 to 60 nm, and 23% coarse grained regions (area fraction) having grain sizes of 0.5–2 μm.

2. Using different combinations of the Cauchy and the Gaussian function approximation to evaluate the XRD profiles, a relative variation of less than 38% for grain size value was obtained. Even though the calculated grain size values from all nine of the approximations are less than 100 nm with very high linear correlation coefficients of 0.97–0.99, the XRD technique is not suitable for the analysis of a bimodal grain microstructure. The inability of XRD analysis to predict the grain size of a material with a bimodal grain size distribution results from the fact that coarse grains do not produce measurable profile broadening.

3. When the coefficient k is selected as 0.742, rather than the traditional value of 0.89, the grain size values calculated on the basis of the full width at half maximum intensity are very close to those calculated on the basis of the integral width (the variation is less than 5%), for all nine of the Cauchy and Gaussian function approximations.

4. TEM studies, combining examination at low and high magnifications, provided a straightforward, quantitative description of the grain size distribution in cryomilled powders having an inhomogeneous distribution in grain size.

Acknowledgements

The present project was financially supported by the Office of Naval Research under Grants N00014-02-1-1053, N00014-03-1-0149 and N00014-03-C-0163, and the Army Research Office under Grant ARO DAAD 19-03-0020.

References

1. H. P. KLUG and L. E. ALEXANDER, "X-ray Diffraction Procedures" (John Wiley & Sons, New York, 1974) p. 634.
2. C. E. KRILL and R. BIRRINGER, *Phil. Mag.* A **77** (1998) 621.
3. H. G. JIANG, M. RUHLE and E. J. LAVERNIA, *J. Mater. Res.* **14** (1999) 549.
4. H. H. TIAN and M. ATZMON, *Phil. Mag.* A **79** (1999) 1769.
5. T. UNGAR, S. OTT, P. G. SANDERS, A. BORBELY and J. R. WEERTMAN, *Acta Materialia* **46** (1998) 3693.
6. C. SURYANARAYANA, *Int. Mat. Rev.* **40** (1995) 41.
7. J. HE, M. ICE, S. DALLEK and E. J. LAVERNIA, *Metall. Mater. Trans.* A **31A** (2000) 541.
8. J. HE, M. ICE and E. J. LAVERNIA, *ibid.* **31A** (2000) 555.
9. J. HE and J. M. SCHOENUNG, *ibid.* **34A** (2003) 673.
10. *Idem.*, *Mater. Sci. Eng.* A **336** (2002) 274.
11. J. HE and E. J. LAVERNIA, *J. Mater. Res.* **16** (2001) 2724.
12. J. S. BENJAMIN, *Metall. Trans.* **1** (1970) 2943.
13. V. L. TELLKAMP, A. MELMED and E. J. LAVERNIA, *Metall. Mater. Trans.* A **32A** (2001) 2335.
14. D. WITKIN, Z. LEE, R. RODRIGUEZ, S. NUTT and E. J. LAVERNIA, "Bulk Nanostructured Al-Mg Alloy for High Strength and Increased Ductility," *Scripta Materialia*, accepted, 2003.
15. Y. M. WANG, M. W. CHEN, F. H. ZHOU and E. MA, *Nature* **419**(6910) (2002) 912.
16. J. HE, K. H. CHUNG, X. LIAO, Y. T. ZHU and E. J. LAVERNIA, *Metall. Mater. Trans.* A **34** (2003) 707.
17. ZONGHOON LEE, RODOLFO RODRIGUEZ, ROBERT W. HAYES, ENRIQUE J. LAVERNIA and STEVEN R. NUTT, "Microstructural Evolution and Deformation of Cryomilled Nanocrystalline Al-Ti-Cu alloy," submitted to *Acta Meter.* 2003.
18. B. D. CULLITY, in "Elements of X-ray Diffraction," 2nd ed. (Addison-Wesley Publishing Company, Inc., Reading, MA, 1978) p. 134, 292, 512.

Received 6 November 2003
and accepted 2 August 2004